Available online at www.eccomasproceedia.org
Eccomas Proceedia COMPDYN (2017) 500-508

ECCOMAS
Proceedia

COMPDYN 2017
6th ECCOMAS Thematic Conference on
Computational Methods in Structural Dynamics and Earthquake Engineering
M. Papadrakakis, M. Fragiadakis (eds.)
Rhodes Island, Greece, 15–17 June, 2017

SENSITIVITY ANALYSIS OF THE FREE WAVE CHARACTERISTICS OF PERIODIC STRUCTURES

Jie Zhang, Guido De Roeck, Edwin Reynders, and Geert Lombaert

KU Leuven, Department of Civil Engineering, Structural Mechanics Section
Kasteelpark Arenberg 40, 3001 Leuven, Belgium
{jie.zhang, guido.deroeck, edwin.reynders, geert.lombaert}@kuleuven.be

Keywords: Sensitivity analysis, free wave, periodic structure

Abstract. *The free wave characteristics, i.e. propagation constants and free waves, characterize the dynamic behaviour of periodic structures. For this reason, they may therefore provide a viable alternative to modal characteristics for finite element model updating. The sensitivities of the free wave characteristics to model parameters are required when using a gradient-based optimization algorithm for model updating. This paper investigates the sensitivity of the free wave characteristics to the model parameters. In this paper, an analytical expression of the sensitivities is derived and verified by comparison to results obtained by finite differences in a case study. The resulting sensitivities are compared to those of the modal characteristics to check their use in finite element model updating. In the case considered, the sensitivities of free wave characteristics are higher than those of the corresponding modal characteristics, indicating that free wave characteristics may be an alternative for model updating.*

Peer-review under responsibility of the organizing committee of COMPDYN 2017.
doi: 10.7712/120117.5435.17400

1 INTRODUCTION

Modal characteristics, i.e. natural frequencies and mode shapes, are generally used as the data features in vibration-based updating of finite element models of civil engineering structures [1]. In the model updating process, unknown or poorly known parameters are determined by minimizing a least-squares cost function. The minimization problem is usually solved by a gradient-based optimization algorithm, requiring the sensitivities of the modal characteristics to the updating parameters. These sensitivities are also used in damage detection and optimal sensor placement for parameter estimation [2].

For periodic structures, the free wave characteristics, i.e. propagation constants and free waves, can be used as an alternative to represent the dynamic behaviour of the structure [3]. Therefore it might be possible to use free wave characteristics, instead of modal characteristics, as data features in model updating of periodic structures.

This paper investigates the sensitivity of the free wave characteristics to model parameters. The free wave characteristics are calculated from the solution of an eigenvalue problem. The derivatives of eigenvalues and eigenvectors have been extensively studied [4, 5, 6]. An analytical expression of the sensitivities is derived following Nelson's method [5, 6], which is an adjoint method. The expressions are verified by comparison to results obtained by finite differences in a case study considering an infinite periodic frame structure. The resulting sensitivities are compared to those of the modal characteristics to check their use in finite element model updating.

2 FREE WAVE CHARACTERISTICS

Figure 1a shows an example of a repetitive frame structure, consisting of identical repetitive units shown in figure 1b. The unit contains the internal DOFs (Ω) and the interface DOFs (Γ_{L}, Γ_{R}) which are coupled with the adjacent units. The free wave characteristics can be calculated by analyzing a single unit [3].

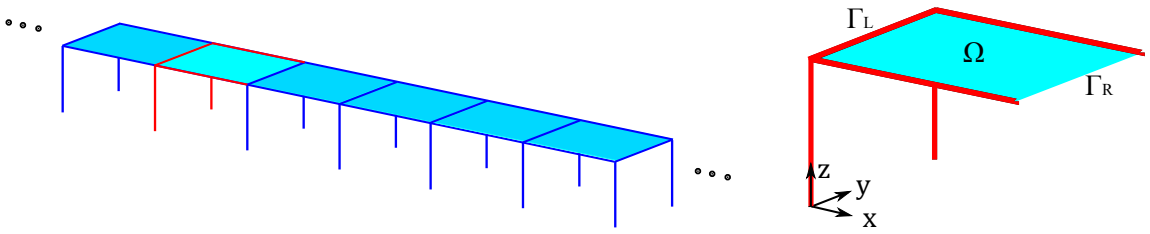

(a) (b)

Figure 1: (a) An infinite repetitive frame structure, (b) a repetitive unit.

The equation of motion of one unit in the frequency domain is:

$$\begin{bmatrix} \hat{\mathbf{F}}_{\mathrm{L}} \\ \mathbf{0} \\ \hat{\mathbf{F}}_{\mathrm{R}} \end{bmatrix} = \begin{bmatrix} \mathbf{D}_{\mathrm{LL}} & \mathbf{D}_{\mathrm{Li}} & \mathbf{D}_{\mathrm{LR}} \\ \mathbf{D}_{\mathrm{iL}} & \mathbf{D}_{\mathrm{ii}} & \mathbf{D}_{\mathrm{iR}} \\ \mathbf{D}_{\mathrm{RL}} & \mathbf{D}_{\mathrm{Ri}} & \mathbf{D}_{\mathrm{RR}} \end{bmatrix} \begin{bmatrix} \hat{\mathbf{u}}_{\mathrm{L}} \\ \hat{\mathbf{u}}_{\mathrm{i}} \\ \hat{\mathbf{u}}_{\mathrm{R}} \end{bmatrix} \tag{1}$$

where $\mathbf{D}$ is the dynamic stiffness matrix, $\hat{\mathbf{F}}$ is the force acting on the unit and $\mathbf{u}$ is the displacement. Subscripts i, L and R represent DOFs at Ω, Γ_{L} and Γ_{R} respectively. $\hat{\mathbf{F}}_{\mathrm{L}}$ and $\hat{\mathbf{F}}_{\mathrm{R}}$ are forces transferred at the interfaces. For the calculation of the free wave characteristics, there are no external forces acting on the internal DOFs Ω.

The equation of motion can be written in a reduced form by considering the DOFs at Γ_{L} and Γ_{R} only:

$$\begin{bmatrix}\hat{\mathbf{F}}_{\mathrm{L}}\\ \hat{\mathbf{F}}_{\mathrm{R}}\end{bmatrix} = \begin{bmatrix}\underline{\mathbf{D}}_{\mathrm{LL}} & \underline{\mathbf{D}}_{\mathrm{LR}}\\ \underline{\mathbf{D}}_{\mathrm{RL}} & \underline{\mathbf{D}}_{\mathrm{RR}}\end{bmatrix}\begin{bmatrix}\hat{\mathbf{u}}_{\mathrm{L}}\\ \hat{\mathbf{u}}_{\mathrm{R}}\end{bmatrix} \tag{2}$$

where

$$\underline{\mathbf{D}}_{\mathrm{LL}} = \mathbf{D}_{\mathrm{LL}} - \mathbf{D}_{\mathrm{Li}}\mathbf{D}_{\mathrm{ii}}^{-1}\mathbf{D}_{\mathrm{iL}} \tag{3a}$$
$$\underline{\mathbf{D}}_{\mathrm{LR}} = \mathbf{D}_{\mathrm{LR}} - \mathbf{D}_{\mathrm{Li}}\mathbf{D}_{\mathrm{ii}}^{-1}\mathbf{D}_{\mathrm{iR}} \tag{3b}$$
$$\underline{\mathbf{D}}_{\mathrm{RL}} = \mathbf{D}_{\mathrm{RL}} - \mathbf{D}_{\mathrm{Ri}}\mathbf{D}_{\mathrm{ii}}^{-1}\mathbf{D}_{\mathrm{iL}} \tag{3c}$$
$$\underline{\mathbf{D}}_{\mathrm{RR}} = \mathbf{D}_{\mathrm{RR}} - \mathbf{D}_{\mathrm{Ri}}\mathbf{D}_{\mathrm{ii}}^{-1}\mathbf{D}_{\mathrm{iR}} \tag{3d}$$

The propagation constants and free wave vectors are obtain by solving the following eigenvalue problem:

$$[\underline{\mathbf{D}}_{\mathrm{LR}}e^{2\mu} + (\underline{\mathbf{D}}_{\mathrm{LL}} + \underline{\mathbf{D}}_{\mathrm{RR}})e^{\mu} + \underline{\mathbf{D}}_{\mathrm{RL}}]\{\hat{\mathbf{u}}_{\mathrm{L}}\} = \mathbf{0} \tag{4}$$

n_{c} pairs of free waves are obtained with n_{c} the number of the coupling DOFs. Each pair contains one positive going free wave ($\boldsymbol{\psi}_{\mathrm{p}k}$) and one identical but negative going free wave ($\boldsymbol{\psi}_{\mathrm{n}k}$), characterized by a negative ($\mu_{\mathrm{p}k}$) and a positive propagation constant ($\mu_{\mathrm{n}k} = -\mu_{\mathrm{p}k}$), respectively. The subscripts p and n represents positive going and negative going free waves, and k denotes the k^{th} pair of free waves.

3 SENSITIVITIES OF THE FREE WAVE CHARACTERISTICS

Following the method of Nelson [5, 6], the first derivatives of the eigenvalues and eigenvectors are calculated. For simplification, the eigenvalue problem in equation (4) is written as:

$$[\mathbf{A}\lambda^2 + \mathbf{B}\lambda + \mathbf{C}]\boldsymbol{\psi} = \mathbf{0} \tag{5}$$

where $\mathbf{A} = \underline{\mathbf{D}}_{\mathrm{LR}}, \mathbf{B} = \underline{\mathbf{D}}_{\mathrm{LL}} + \underline{\mathbf{D}}_{\mathrm{RR}}, \mathbf{C} = \underline{\mathbf{D}}_{\mathrm{RL}}$ and $\lambda = e^{\mu}$.

The first derivatives of the eigenvalues and eigenvectors are calculated for the non-self-adjoint case [6], which is briefly introduced as follows. The k^{th} positive going free wave ($\lambda_{\mathrm{p}k}$, $\boldsymbol{\psi}_{\mathrm{p}k}$) is used to demonstrate the procedure.

For the k^{th} left ($\boldsymbol{\phi}_{\mathrm{p}k}$) and right ($\boldsymbol{\psi}_{\mathrm{p}k}$) eigenvector, the eigenvalue problems are written as:

$$[\mathbf{A}\lambda_{\mathrm{p}k}^2 + \mathbf{B}\lambda_{\mathrm{p}k} + \mathbf{C}]\boldsymbol{\psi}_{\mathrm{p}k} = \mathbf{0} \tag{6a}$$
$$\boldsymbol{\phi}_{\mathrm{p}k}^{\mathrm{T}}[\mathbf{A}\lambda_{\mathrm{p}k}^2 + \mathbf{B}\lambda_{\mathrm{p}k} + \mathbf{C}] = \mathbf{0} \tag{6b}$$

The eigenvectors are normalized following equations (7a) and (7b):

$$\boldsymbol{\phi}_{\mathrm{p}k}^{\mathrm{T}}(2\lambda_{\mathrm{p}k}\mathbf{A} + \mathbf{B})\boldsymbol{\psi}_{\mathrm{p}k} = 1 \tag{7a}$$
$$\{\boldsymbol{\phi}_{\mathrm{p}k}\}_j = \{\boldsymbol{\psi}_{\mathrm{p}k}\}_j \tag{7b}$$

where the subscript j denotes the j^{th} element in the eigenvector, j is preferably chosen as the location where both the left and the right eigenvector have a large magnitude. Equation (8) also holds:

$$\{\frac{\partial\boldsymbol{\psi}_{\mathrm{p}k}}{\partial\theta}\}_j = \{\frac{\partial\boldsymbol{\phi}_{\mathrm{p}k}}{\partial\theta}\}_j \tag{8}$$

By differentiating equation (6a) with respect to the model parameter θ, the following equation is obtained:

$$(\lambda_{\mathrm{p}k}^2\frac{\partial \mathbf{A}}{\partial \theta}+\lambda_{\mathrm{p}k}\frac{\partial \mathbf{B}}{\partial \theta}+\frac{\partial \mathbf{C}}{\partial \theta})\boldsymbol{\psi}_{\mathrm{p}k}+(2\lambda_{\mathrm{p}k}\mathbf{A}+\mathbf{B})\boldsymbol{\psi}_{\mathrm{p}k}\frac{\partial \lambda_{\mathrm{p}k}}{\partial \theta}+(\lambda_{\mathrm{p}k}^2\mathbf{A}+\lambda_{\mathrm{p}k}\mathbf{B}+\mathbf{C})\frac{\partial \boldsymbol{\psi}_{\mathrm{p}k}}{\partial \theta}=0 \quad (9)$$

Premultiplied by $\boldsymbol{\phi}_{\mathrm{p}k}^{\mathrm{T}}$, equation (9) becomes:

$$\boldsymbol{\phi}_{\mathrm{p}k}^{\mathrm{T}}(\lambda_{\mathrm{p}k}^2\frac{\partial \mathbf{A}}{\partial \theta}+\lambda_{\mathrm{p}k}\frac{\partial \mathbf{B}}{\partial \theta}+\frac{\partial \mathbf{C}}{\partial \theta})\boldsymbol{\psi}_{\mathrm{p}k}+\boldsymbol{\phi}_{\mathrm{p}k}^{\mathrm{T}}(2\lambda_{\mathrm{p}k}\mathbf{A}+\mathbf{B})\boldsymbol{\psi}_{\mathrm{p}k}\frac{\partial \lambda_{\mathrm{p}k}}{\partial \theta}+\boldsymbol{\phi}_{\mathrm{p}k}^{\mathrm{T}}(\lambda_{\mathrm{p}k}^2\mathbf{A}+\lambda_{\mathrm{p}k}\mathbf{B}+\mathbf{C})\frac{\partial \boldsymbol{\psi}_{\mathrm{p}k}}{\partial \theta}=0 \quad (10)$$

where the third term is equal to 0 and $\boldsymbol{\phi}_{\mathrm{p}k}^{\mathrm{T}}(2\lambda_{\mathrm{p}k}\mathbf{A}+\mathbf{B})\boldsymbol{\psi}_{\mathrm{p}k}$ in the second term is equal to 1 due to the normalization.

The first derivative of the eigenvalue is calculated from equation (10):

$$\frac{\partial \lambda_{\mathrm{p}k}}{\partial \theta}=-\boldsymbol{\phi}_{\mathrm{p}k}^{\mathrm{T}}(\lambda_{\mathrm{p}k}^2\frac{\partial \mathbf{A}}{\partial \theta}+\lambda_{\mathrm{p}k}\frac{\partial \mathbf{B}}{\partial \theta}+\frac{\partial \mathbf{C}}{\partial \theta})\boldsymbol{\psi}_{\mathrm{p}k} \quad (11)$$

The calculation requires the sensitivities of matrices $\mathbf{A}$, $\mathbf{B}$ and $\mathbf{C}$:

$$\frac{\partial \mathbf{A}}{\partial \theta}=\frac{\partial \mathbf{D}_{\mathrm{LR}}}{\partial \theta}-\frac{\partial \mathbf{D}_{\mathrm{Li}}}{\partial \theta}\mathbf{D}_{\mathrm{ii}}^{-1}\mathbf{D}_{\mathrm{iR}}+\mathbf{D}_{\mathrm{Li}}\mathbf{D}_{\mathrm{ii}}^{-1}\frac{\partial \mathbf{D}_{\mathrm{ii}}}{\partial \theta}\mathbf{D}_{\mathrm{ii}}^{-1}\mathbf{D}_{\mathrm{iR}}-\mathbf{D}_{\mathrm{Li}}\mathbf{D}_{\mathrm{ii}}^{-1}\frac{\partial \mathbf{D}_{\mathrm{iR}}}{\partial \theta} \quad (12)$$

$$\begin{aligned}\frac{\partial \mathbf{B}}{\partial \theta}=&\frac{\partial \mathbf{D}_{\mathrm{LL}}}{\partial \theta}-\frac{\partial \mathbf{D}_{\mathrm{Li}}}{\partial \theta}\mathbf{D}_{\mathrm{ii}}^{-1}\mathbf{D}_{\mathrm{iL}}+\mathbf{D}_{\mathrm{Li}}\mathbf{D}_{\mathrm{ii}}^{-1}\frac{\partial \mathbf{D}_{\mathrm{ii}}}{\partial \theta}\mathbf{D}_{\mathrm{ii}}^{-1}\mathbf{D}_{\mathrm{iL}}-\mathbf{D}_{\mathrm{Li}}\mathbf{D}_{\mathrm{ii}}^{-1}\frac{\partial \mathbf{D}_{\mathrm{iL}}}{\partial \theta}\\&+\frac{\partial \mathbf{D}_{\mathrm{RR}}}{\partial \theta}-\frac{\partial \mathbf{D}_{\mathrm{Ri}}}{\partial \theta}\mathbf{D}_{\mathrm{ii}}^{-1}\mathbf{D}_{\mathrm{iR}}+\mathbf{D}_{\mathrm{Ri}}\mathbf{D}_{\mathrm{ii}}^{-1}\frac{\partial \mathbf{D}_{\mathrm{ii}}}{\partial \theta}\mathbf{D}_{\mathrm{ii}}^{-1}\mathbf{D}_{\mathrm{iR}}-\mathbf{D}_{\mathrm{Ri}}\mathbf{D}_{\mathrm{ii}}^{-1}\frac{\partial \mathbf{D}_{\mathrm{iR}}}{\partial \theta}\end{aligned} \quad (13)$$

$$\frac{\partial \mathbf{C}}{\partial \theta}=\frac{\partial \mathbf{D}_{\mathrm{RL}}}{\partial \theta}-\frac{\partial \mathbf{D}_{\mathrm{Ri}}}{\partial \theta}\mathbf{D}_{\mathrm{ii}}^{-1}\mathbf{D}_{\mathrm{iL}}+\mathbf{D}_{\mathrm{Ri}}\mathbf{D}_{\mathrm{ii}}^{-1}\frac{\partial \mathbf{D}_{\mathrm{ii}}}{\partial \theta}\mathbf{D}_{\mathrm{ii}}^{-1}\mathbf{D}_{\mathrm{iL}}-\mathbf{D}_{\mathrm{Ri}}\mathbf{D}_{\mathrm{ii}}^{-1}\frac{\partial \mathbf{D}_{\mathrm{iL}}}{\partial \theta} \quad (14)$$

The first derivative of the eigenvectors are calculated as the sum of the particular and the homogeneous solution:

$$\frac{\partial \boldsymbol{\psi}_{\mathrm{p}k}}{\partial \theta}=\mathbf{x}_{\mathrm{p}k}+c_{\mathrm{p}k}\boldsymbol{\psi}_{\mathrm{p}k} \quad (15a)$$

$$\frac{\partial \boldsymbol{\phi}_{\mathrm{p}k}}{\partial \theta}=\mathbf{y}_{\mathrm{p}k}+d_{\mathrm{p}k}\boldsymbol{\phi}_{\mathrm{p}k} \quad (15b)$$

where $\mathbf{x}_{\mathrm{p}k}$, $\mathbf{y}_{\mathrm{p}k}$, $c_{\mathrm{p}k}$ and $d_{\mathrm{p}k}$ are to be determined. $\mathbf{x}_{\mathrm{p}k}$ is calculated from equation (16) by substituting equation (15a) into equation (9) and making the l^{th} element in $\mathbf{x}_{\mathrm{p}k}$ equal to 0. l is preferably taken as the location where $\boldsymbol{\psi}_{\mathrm{p}k}$ has the largest magnitude. $\mathbf{y}_{\mathrm{p}k}$ is calculated in a similar way.

$$(\lambda_{\mathrm{p}k}^2\mathbf{A}+\lambda_{\mathrm{p}k}\mathbf{B}+\mathbf{C})\mathbf{x}_{\mathrm{p}k}=-(\lambda_{\mathrm{p}k}^2\frac{\partial \mathbf{A}}{\partial \theta}+\lambda_{\mathrm{p}k}\frac{\partial \mathbf{B}}{\partial \theta}+\frac{\partial \mathbf{C}}{\partial \theta})\boldsymbol{\psi}_{\mathrm{p}k}-(2\lambda_{\mathrm{p}k}\mathbf{A}+\mathbf{B})\boldsymbol{\psi}_{\mathrm{p}k}\frac{\partial \lambda_{\mathrm{p}k}}{\partial \theta} \quad (16)$$

By differentiating equation (7a), equation (17) is obtained.

$$\boldsymbol{\phi}_{\mathrm{p}k}^{\mathrm{T}}(2\lambda_{\mathrm{p}k}\mathbf{A}+\mathbf{B})\frac{\partial \boldsymbol{\psi}_{\mathrm{p}k}}{\partial \theta}+\frac{\partial \boldsymbol{\phi}_{\mathrm{p}k}^{\mathrm{T}}}{\partial \theta}(2\lambda_{\mathrm{p}k}\mathbf{A}+\mathbf{B})\boldsymbol{\psi}_{\mathrm{p}k}+\boldsymbol{\phi}_{\mathrm{p}k}^{\mathrm{T}}(2\mathbf{A}\frac{\partial \lambda_{\mathrm{p}k}}{\partial \theta}+2\lambda_{\mathrm{p}k}\frac{\partial \mathbf{A}}{\partial \theta}+\frac{\partial \mathbf{B}}{\partial \theta})\boldsymbol{\psi}_{\mathrm{p}k}=0 \quad (17)$$

An equation for $c_{\mathrm{p}k}$ and $d_{\mathrm{p}k}$ are obtained by substituting equations (15a) and (15b) into equation (17):

$$c_{\mathrm{p}k}+d_{\mathrm{p}k} = -\boldsymbol{\phi}_{\mathrm{p}k}^{\mathrm{T}}(2\lambda_{\mathrm{p}k}\mathbf{A}+\mathbf{B})\mathbf{x}_{\mathrm{p}k}-\mathbf{y}_{\mathrm{p}k}^{\mathrm{T}}(2\lambda_{\mathrm{p}k}\mathbf{A}+\mathbf{B})\boldsymbol{\psi}_{\mathrm{p}k}-\boldsymbol{\phi}_{\mathrm{p}k}^{\mathrm{T}}(2\mathbf{A}\frac{\partial\lambda_{\mathrm{p}k}}{\partial\theta}+2\lambda_{\mathrm{p}k}\frac{\partial\mathbf{A}}{\partial\theta}+\frac{\partial\mathbf{B}}{\partial\theta})\boldsymbol{\psi}_{\mathrm{p}k} \tag{18}$$

Another equation for $c_{\mathrm{p}k}$ and $d_{\mathrm{p}k}$ are obtained by substituting the j^{th} element in equation (15a) and equation (15b) into equations (7b) and (8):

$$(c_{\mathrm{p}k}-d_{\mathrm{p}k})\{\boldsymbol{\psi}_{\mathrm{p}k}\}_j = \{\mathbf{y}_{\mathrm{p}k}\}_j - \{\mathbf{x}_{\mathrm{p}k}\}_j \tag{19}$$

$c_{\mathrm{p}k}$ and $d_{\mathrm{p}k}$ are calculated from these two equations.

Introducing $\mathbf{x}_{\mathrm{p}k}$, $\mathbf{y}_{\mathrm{p}k}$, $c_{\mathrm{p}k}$ and $d_{\mathrm{p}k}$ in equations (15a) and (15b), the derivatives of the eigenvectors can be calculated.

4 APPLICATION

The modal characteristics are calculated for the repetitive frame structure with 6 bays (figure 2a). The structure consists of concrete slabs, beams and columns. The floor of one bay has a dimension of $5\ \mathrm{m} \times 5\ \mathrm{m}$ and a thickness of $0.15\ \mathrm{m}$. The beams and columns have a rectangular section of $0.2\ \mathrm{m} \times 0.5\ \mathrm{m}$ and $0.35\ \mathrm{m} \times 0.35\ \mathrm{m}$, respectively. The story height is 3 m. The concrete has a elastic modulus of $E = 35 \times 10^9\ \mathrm{N/m^2}$ and a density of $\rho = 2500\ \mathrm{kg/m^3}$. The structure is analyzed using StaBIL, a finite element toolbox in MATLAB developed by the Structural Mechanics Section of KU Leuven [7]. The finite element mesh is shown in figure 2b. The modes in the frequency range of 14.0 Hz - 15.3 Hz are plotted in figure 3. In this frequency range, clustered vertical bending modes with closely spaced natural frequencies and similar wavelengths occur [8].

The free wave characteristics in the infinite frame structure are calculated from the repetitive unit shown in figure 1b at 15.15 Hz, which is the 8^{th} natural frequency of the 6-bay structure. The sensitivities of the free waves at this frequency will be compared to those of the 8^{th} mode.

In the absence of damping, there are three pairs of non-decaying waves at this frequency, while the other waves are decaying. Figure 4a-4c illustrates the three positive going non-decaying waves for a finite part of the infinite structure, including a longitudinal wave, a lateral bending wave and a vertical bending wave. As an example, three of the positive going decaying waves are shown in figure 4d-4f, including one vertical bending wave, one lateral bending wave and one local floor bending wave.

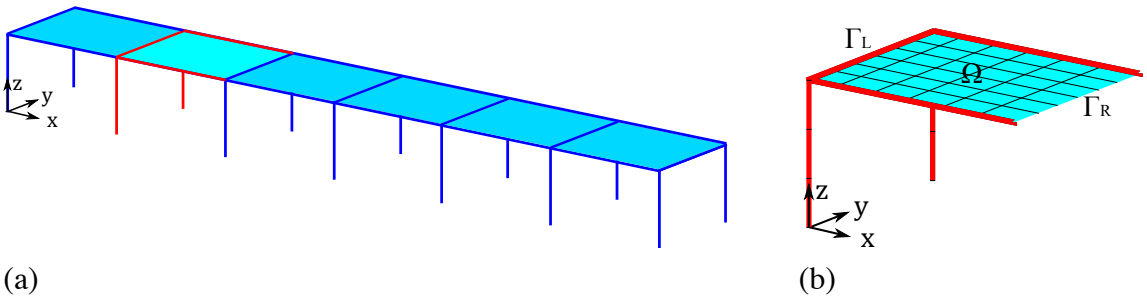

(a) (b)

Figure 2: (a) The 6-bay repetitive frame structure, (b) the mesh of one unit.

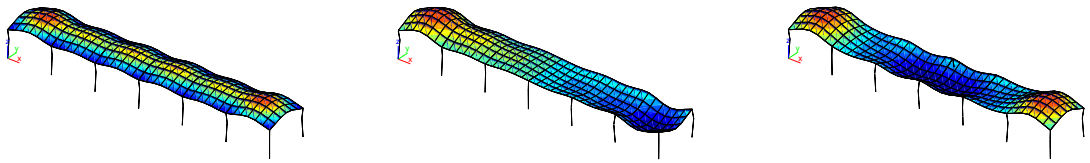

(a) mode 4, 14.13 Hz (b) mode 5, 14.24 Hz (c) mode 6, 14.52 Hz

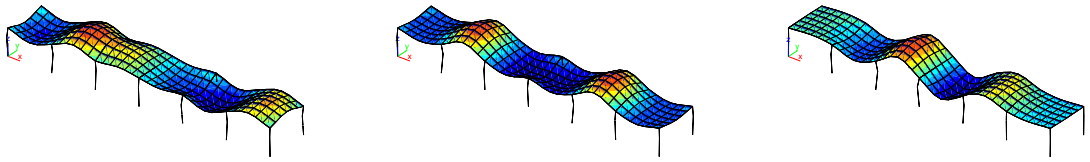

(d) mode 7, 14.87 Hz (e) mode 8, 15.15 Hz (f) mode 9, 15.23 Hz

Figure 3: The modes in the frequency range of 14.0 Hz - 15.3 Hz.

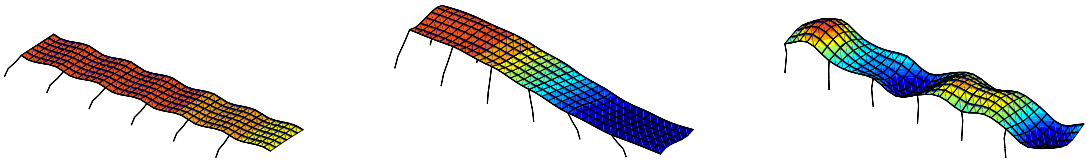

(a) $\mu_{\mathrm{p}1} = -0.1227i$ (b) $\mu_{\mathrm{p}2} = -0.6243i$ (c) $\mu_{\mathrm{p}3} = -1.8097i$

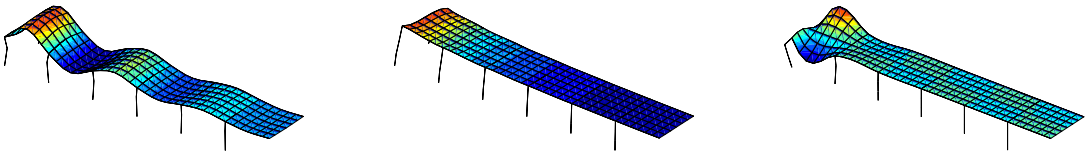

(d) $\mu_{\mathrm{p}4} = -0.4523 + 3.1416i$ (e) $\mu_{\mathrm{p}5} = 0.5730$ (f) $\mu_{\mathrm{p}6} = -2.0203 + 3.1416i$

Figure 4: The free waves at 15.15 Hz.

The model parameter θ is taken as a scale factor for the elastic modulus E for the slab ($E_{\mathrm{slab}} = \theta E$). The sensitivities of the free waves at 15.15 Hz to the parameter θ are calculated based on the analytical expressions and compared with those obtained using finite difference method. The sensitivities of the propagation constants and those of the free wave vectors are shown in table 1 and figure 5, respectively. The analytical expressions and the finite difference method give nearly identical results. From table 1, it is found that the sensitivities of the propagation constants for free wave 3 and free wave 4 are larger than those for the other free waves.

	Wave 1	Wave 2	Wave 3	Wave 4	Wave 5	Wave 6
μ_{p}	$-0.1227i$	$-0.6243i$	$-1.8097i$	$-0.4523 + \pi i$	0.5730	$-2.0203 + \pi i$
$\frac{\partial \mu_{\mathrm{p}}}{\partial \theta}$ (analytical)	$0.0499i$	$0.1085i$	$7.8967i$	-11.5718	0.0681	-0.2008
$\frac{\partial \mu_{\mathrm{p}}}{\partial \theta}$ (finite difference)	$0.0499i$	$0.1085i$	$7.8967i$	-11.5718	0.0681	-0.2008

Table 1: The sensitivities of the propagation constants at 15.15 Hz.

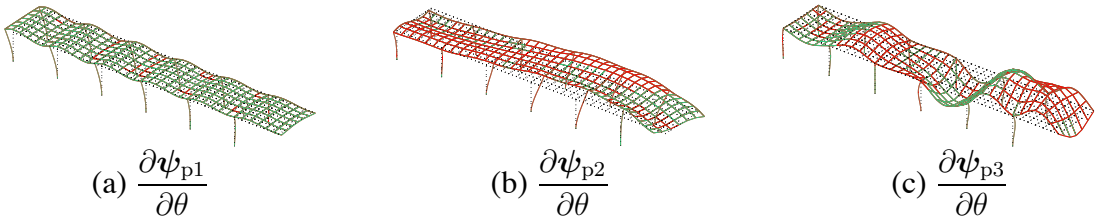

(a) $\frac{\partial \boldsymbol{\psi}_{\mathrm{p1}}}{\partial \theta}$ (b) $\frac{\partial \boldsymbol{\psi}_{\mathrm{p2}}}{\partial \theta}$ (c) $\frac{\partial \boldsymbol{\psi}_{\mathrm{p3}}}{\partial \theta}$

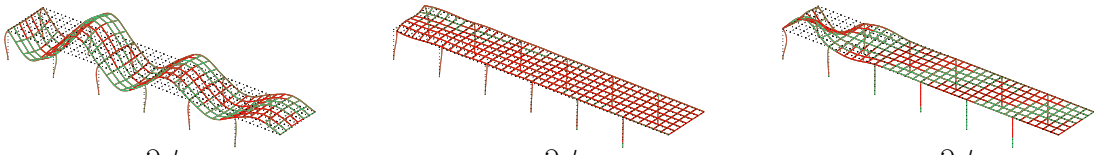

(d) $\frac{\partial \boldsymbol{\psi}_{\mathrm{p4}}}{\partial \theta}$ (e) $\frac{\partial \boldsymbol{\psi}_{\mathrm{p5}}}{\partial \theta}$ (f) $\frac{\partial \boldsymbol{\psi}_{\mathrm{p6}}}{\partial \theta}$

Figure 5: The sensitivities of the free waves at 15.15 Hz obtained from the analytical expressions (red) and the finite difference method (green).

In order to have a physical understanding of how sensitive a free wave is to the parameter θ, the changes in the free wave characteristics are studied for a small perturbation on θ. With a small perturbation on θ, the changes in the propagation constants and the free wave vectors are approximately written as:

$$\Delta\mu_{\mathrm{p}k} \approx \frac{\partial \mu_{\mathrm{p}k}}{\partial \theta}\Delta\theta \tag{20a}$$

$$\Delta\boldsymbol{\psi}_{\mathrm{p}k} \approx \frac{\partial \boldsymbol{\psi}_{\mathrm{p}k}}{\partial \theta}\Delta\theta \tag{20b}$$

The changes of the free waves are plotted in figure 6 and compared to the free waves for a perturbation $\Delta\theta = 0.1$, corresponding to a 10% increase in the elastic modulus of the slab. The same scale is used for the changes ($\Delta\boldsymbol{\psi}_{\mathrm{p}k}$) and the corresponding free waves ($\boldsymbol{\psi}_{\mathrm{p}k}$). It can be seen that free wave 3 and free wave 4 are much more sensitive to θ than the other free waves. The changes in the propagation constants of free wave 3 and free wave 4 are also larger than those of the other free waves. The elastic modulus of the slabs has a larger influence on these two free waves as they involve vertical bending of the floor.

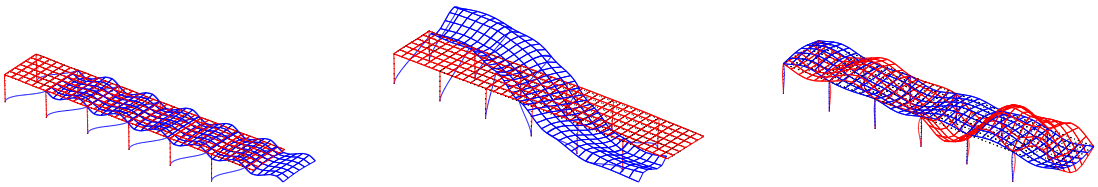

(a) $\Delta\boldsymbol{\psi}_{\mathrm{p1}}$ ($\Delta\mu_{\mathrm{p1}} = 0.0050i$) (b) $\Delta\boldsymbol{\psi}_{\mathrm{p2}}$ ($\Delta\mu_{\mathrm{p2}} = 0.0109i$) (c) $\Delta\boldsymbol{\psi}_{\mathrm{p3}}$ ($\Delta\mu_{\mathrm{p3}} = 0.7897i$)

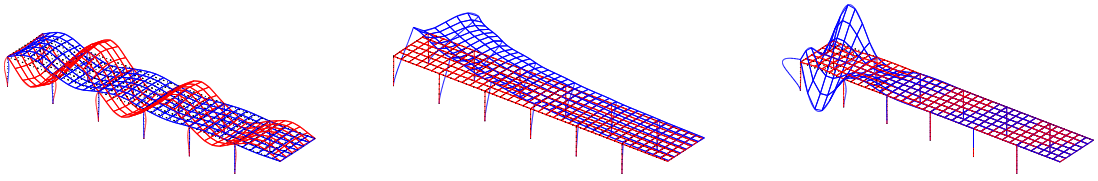

(d) $\Delta\boldsymbol{\psi}_{\mathrm{p4}}$ ($\Delta\mu_{\mathrm{p4}} = 1.1572$) (e) $\Delta\boldsymbol{\psi}_{\mathrm{p5}}$ ($\Delta\mu_{\mathrm{p5}} = 0.0068$) (f) $\Delta\boldsymbol{\psi}_{\mathrm{p6}}$ ($\Delta\mu_{\mathrm{p6}} = 0.0201$)

Figure 6: The changes (red) in the corresponding free waves (blue) at 15.15 Hz with $\Delta\theta = 0.1$.

The vertical bending mode shape at 15.15 Hz and the changes in this mode shape with $\Delta\theta = 0.1$ are plotted in figure 7. The change in the 8^{th} natural frequency is $\Delta f = 0.4$ Hz relative to $f = 15.15$ Hz. Compared to the 3^{rd} and 4^{th} free wave, which also involve vertical bending of the floor, the mode shape is less sensitive to the parameter θ.

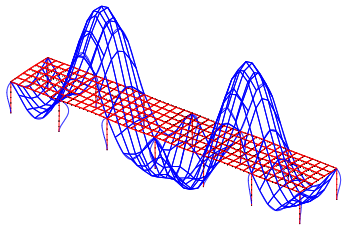

Figure 7: The changes (red) in the corresponding mode shape (blue) at 15.15 Hz with $\Delta\theta = 0.1$.

5 CONCLUSIONS

The analytical expressions of the sensitivities of the free wave characteristics are derived. In the case of the frame structure considered, the free wave characteristics are found to be more sensitive than the modal characteristics. This suggests that the free wave characteristics may be a viable alternative to the modal characteristics for finite element model updating.

6 ACKNOWLEDGMENTS

The research presented in this paper has been performed within the framework of project OT/13/59 “Quantifying and reducing uncertainty in structural dynamics”, funded by the Research Council of KU Leuven. The financial support of KU Leuven is gratefully acknowledged. The second, third and last author are members of the KU Leuven-BOF PFV/10/002 OPTEC-Optimization in Engineering Center.

REFERENCES

[1] E. Simoen, G. Lombaert, and G. De Roeck, Dealing with uncertainty in model updating for damage assessment: a review. *Mechanical Systems and Signal Processing*, **56-57**, 123–149, 2015.

[2] C. Papadimitriou, G. Lombaert, The effect of prediction error correlation on optimal sensor placement in structural dynamics. *Mechanical Systems and Signal Processing*, **28**, 105–127, 2012.

[3] D.J. Mead, A general theory of harmonic wave propagation in linear periodic systems with multiple coupling. *Journal of Sound and Vibration*, **27 (2)**, 235–260, 1973.

[4] R.L. Fox, M.P. Kapoor, Rates of change of eigenvalues and eigenvectors. *AIAA Journal*, **6 (12)**, 2426–2429, 1968.

[5] R.B. Nelson, Simplified calculation of eigenvector derivatives. *AIAA Journal*, **14 (9)**, 1201–1205, 1976.

[6] M.I. Friswell, S. Adhikari, Derivatives of complex eigenvectors using Nelson’s method. *AIAA Journal*, **38 (12)**, 2355–2357, 2000.

[7] D. Dooms, G. De Roeck, G. Degrande, G. Lombaert, M. Schevenels, S. François, StaBIL: A finite element toolbox for MATLAB, Technical Report BWM-2009-20, Department of Civil Engineering, KU Leuven, October 2009.

[8] J. Zhang, G. De Roeck, E. Reynders, G. Lombaert, Optimal sensor placement for modal identification of repetitive structures. *International Conference on Noise and Vibration Engineering (ISMA 2016)*, Leuven, Belgium, 2355–2364, September 19-21, 2016.